

DUAL BAND COPLANAR CAPACITIVE COUPLED MICROSTRIP ANTENNAS WITH AND WITHOUT AIR GAP FOR WIRELESS APPLICATIONS

Veeresh G. Kasabegoudar* and Ajit Kumar

P. G. Department, MBES College of Engineering, Ambajogai 431 517, India

Abstract—This article presents the coplanar capacitive coupled probe fed microstrip antennas for dual frequency band operation. The proposed antenna is excited by a single probe feed connected to a capacitive strip. Of the two dual band antennas presented here, the first one uses small air gap and the other is designed without air gap. In the first case an effort has been made to reduce the height of suspended antenna. A vertical slot is placed to obtain antenna resonance at low frequency side, and also for proper impedance matching. After presenting the basic geometry the second configuration (which uses no air gap) which also offers dual band operation at the expense of reduced bandwidth is presented. Measured values fairly agree with the simulated results.

1. INTRODUCTION

Microstrip antennas are the right candidates for several wireless applications (GSM, Wi-Max, RFID etc.) because of their numerous advantages including easy design and fabrication procedure [1,2]. However, these antennas exhibit a few serious limitations such as low impedance bandwidth and gain in their conventional form. Hence, several researchers reported numerous techniques to improve these restrictions especially enhancing the impedance bandwidth. These alterations include, cutting slots in the basic shapes [3], changing the shape of the geometry [4], or using multi-layer techniques [5]. Bandwidth enhancement can also be achieved by modifying the feed networks (elements) such as meandered probe [6] or changing the

Received 6 November 2012, Accepted 7 January 2013, Scheduled 10 January 2013

* Corresponding author: Veeresh G. Kasabegoudar (veereshgk2002@rediffmail.com).

probe to T-shape [7]. However, many of these geometries use multiple metal/dielectric layers for enhancing the impedance bandwidth which pose fabrication and assembly problems.

On the other hand, single layer suspended microstrip antennas are simple to realize and offer high impedance bandwidth [8–12, 14, 15]. Using this technique a single layer suspended microstrip antenna which offers 50% ($S_{11} < -10$ dB) impedance bandwidth has been reported in [9].

It is well known that considerable bandwidth enhancement can be achieved by increasing the overall height of the composite air-dielectric medium [9–14]. However, the use of air gap increases the height/volume of the antenna which is undesired in several (compact) applications [15]. Therefore, a design that uses small air gap for the similar antenna design is reported earlier [13].

There are several microstrip patch antennas available in literature, which operate at dual resonant frequencies [14, 18–30]. For example antenna reported in [18] uses stacked configuration [18], whereas geometry presented in [19] uses suspended configuration (with air gap) [19]. Other techniques include modified ground shape [20], dual feed [21] etc., which in some cases is contrary to the fundamental attraction of microstrip antennas. On the other hand antenna reported in [22] uses modified probe feed which requires precise alignment.

As stated in above paragraphs, several applications require compact antenna geometries which occupy small area/volume of the wireless device. Hence, in this work we propose a design that uses small air gap for the similar antenna designs reported earlier. The antenna developed here is suitable for various wireless applications like ISM (2.4–2.5 GHz), PCS cellular spectrum widely licensed across the US at 1.9 GHz, broadband wireless commercial service delivery in US (2.3 GHz) etc.. In another effort we have designed antenna which uses no air gap and yields dual resonant bands at the expense of reduced bandwidth. However, this configuration is useful where wireless devices operate at fixed resonant frequencies.

The basic geometry and its working are presented in Section 2. The design starts with the selection of center frequency and it may be noted that the design approach can be easily scaled to any frequency of interest [9]. The antenna without air gap is presented in Section 3. Simulation studies to determine the dimensions of the key design parameters and the slot are also presented there. Experimental validation of the basic geometry is presented in Section 4. Conclusions of this study are given in Section 5.

2. BASIC GEOMETRY WITH AIR GAP

The basic geometry of the antenna is shown in Figure 1 [13]. The configuration is basically a suspended microstrip antenna in which radiating patch and the feed strip are etched on the substrate of thickness “ h ” mm. A long pin SMA connector is used to connect the feed strip which couples the energy to a radiating patch by capacitive means. The length and width of the patch are designed for 2 GHz operation as suggested in [9–12]. The radiator patch is loaded with a vertical slot to make the antenna resonant for lower frequencies and for proper matching with the input impedance of the antenna.

The antenna was designed to operate with a center frequency of 2 GHz. Radiator patch dimensions can be calculated from standard design expressions after making necessary corrections for the suspended dielectric [1, 2]. These corrections incorporate the total height above the ground ($g + h$) and effective dielectric constant of the suspended microstrip [16]. It has been shown that the impedance bandwidth of the antenna may be maximized by using the design expression [9]

$$g \cong 0.16\lambda_0 - h\sqrt{\varepsilon_r}. \quad (1)$$

where g is the height of the substrate above the ground, and h and ε_r are the thickness and dielectric constant of the substrate. However, it should be noted that Equation (1) enables us to predict only initial value and the final value may be optimized with the simulation tools like IE3D. The parameters that can be used to optimize the antenna are air gap (g), separation between feed strip and the radiator patch (d), and the feed strip dimensions (length (t) and width (s)).

It may be noted that according to (1) the calculated air gap is 21.3 mm and the optimum air gap reported in [9] is 19.2 mm. In this work we have made an effort to reduce the air gap significantly as suggested in [15]. The new reduced height and feed strip dimensions can be calculated from the empirical relations reported in [15]:

$$g_{\text{modified}} = g_{\text{opt.}} - \Delta g \quad (2)$$

$$s_{\text{modified}} = s_{\text{opt.}} + \Delta s. \quad (3)$$

In (2) and (3), $g_{\text{opt.}}$ and $s_{\text{opt.}}$ are the optimized air gap and feed strip width, respectively, as defined in [9]. And,

$$\Delta s \approx 1.5\Delta g \quad (\Delta g \leq g_{\text{opt.}}/2) \quad (4)$$

$$\Delta s \approx 1.75\Delta g \quad (\Delta g > g_{\text{opt.}}/2). \quad (5)$$

Provided that $s_{\text{modified}} < W$ (width of the radiator patch). Finally, antenna can be optimized for best possible bandwidth within $\pm 5\%$ of these values.

It may also be noted that reducing the air gap in suspended configurations results in the shift of operating band on higher side. This is basically due to increase in the effective dielectric constant of the composite air-dielectric medium. To avoid the frequency shift, a slot has been introduced. It may be recalled that, cutting a slot inside the radiator patch ensures the wide bandwidth [3]. The detailed parametric studies have been reported earlier for the optimization of this geometry [9–11, 13]. Experimental validations (with simulated characteristics) of the geometry are presented in Section 4.

3. GEOMETRY WITHOUT AIR GAP

In another effort the air gap used in antenna geometry shown in Figure 1 is completely removed (Figure 2) for getting dual band operation. However, due to the complete removal of air gap antenna offers narrow bands. This configuration is useful where bandwidth requirement is not the constraint. The substrate used for design and analysis is a glass epoxy material with dielectric constant = 4.4, loss tangent = 0.001, and thickness $h = 3.2$ mm. It may be noted that the substrate used for second geometry (i.e., geometry without air gap) is different from the geometry with air gap. This is done to demonstrate the flexibility of the design. The resonant frequency and the band of operation have been shifted due to different dielectric constant, height of substrate, and absence of air gap. However, this can be redesigned to any frequency of interest as suggested in [9]. The dimensions of the optimized antenna are listed in Table 1.

The length (L) and width (W) of radiator patch may be calculated as suggested in Section 2. Other parameters (t , d , and s) of capacitive

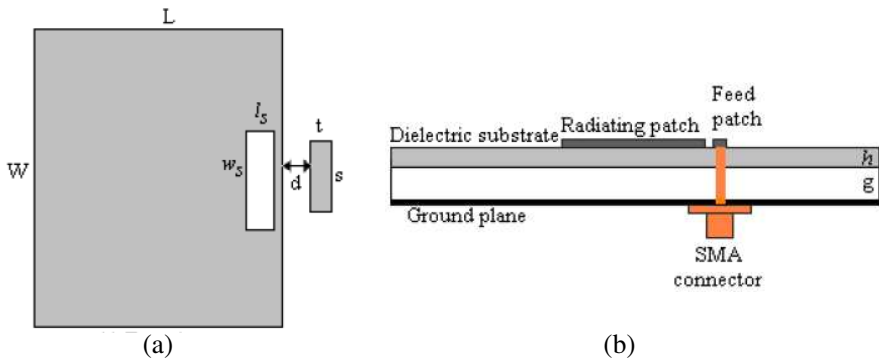


Figure 1. Geometry of a proposed patch antenna with a capacitive feed. (a) Top view. (b) Cross sectional view.

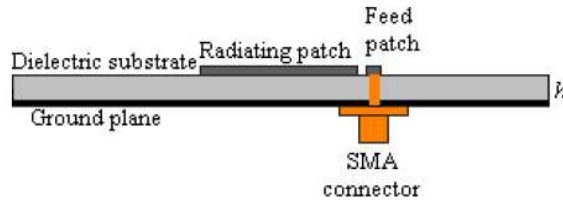


Figure 2. Cross sectional view of a proposed patch antenna without air gap ($g = 0$ and top view remains same as indicated in Figure 1).

Table 1. Optimized dimensions of the proposed antenna with and without air gap.

Antenna Parameter	Values with Air Gap (mm)	Values without Air Gap (mm)
Length of the radiator patch (L)	53.0	46
Width of the radiator patch (W)	80.0	56
Length of the feed strip (s)	9.0	1.2
Width of the feed strip (t)	6.0	16
Separation of feed strip from the patch (d)	0.15	0.2
Air gap (g)	8.5	0
Slot length (l_s)	7.0	6.0
Slot width (w_s)	33.0	32.0
Slot position (p) (from center of patch)	22.5	15.0

feed have been optimized as suggested in [9–12]. It may be noted that initial values of these parameters have been taken from [13] for optimization. Key design parameters (slot position (p), slot width (w_s), and slot length (l_s)) have been investigated to analyze the effect on antenna performance and are discussed in the following subsections.

3.1. Effect of Slot Position (p)

A slot was introduced on the patch to maximize the antenna’s impedance bandwidth [19, 20]. The slot position was varied from 13.0mm to 16.0mm in steps of 1mm with reference to center of the radiating patch. The return loss characteristics of this study are presented in Figure 3. It may be noted that a slot on patch

loads it with capacitive reactance [19, 20]. Detailed analysis of equivalent circuit modeling of capacitive coupled antenna may be found in [11]. Hence, the slot position (p) tunes the input impedance of the antenna by changing the reactive part of input impedance. From the characteristics it may be noted that $p = 15$ mm case exhibits the good resonant characteristics. This parameter not only helps in optimizing the return loss values but also helps in tuning the antenna resonant frequencies (separation between two resonant frequencies). The resonant frequency ratio (f_{r2}/f_{r1}) deviation that can be obtained from the study is from 1.59 to 1.74.

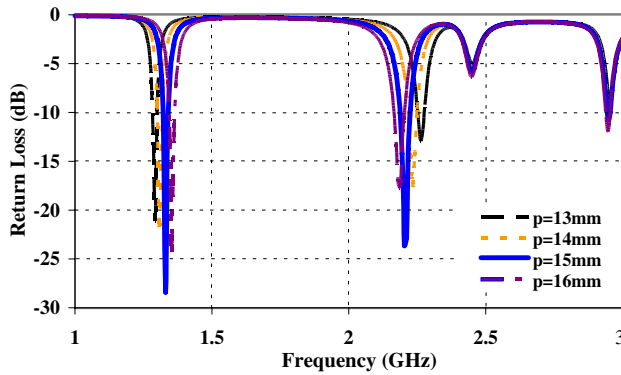


Figure 3. Return loss characteristics for different positions of the slot from the center of the radiating patch.

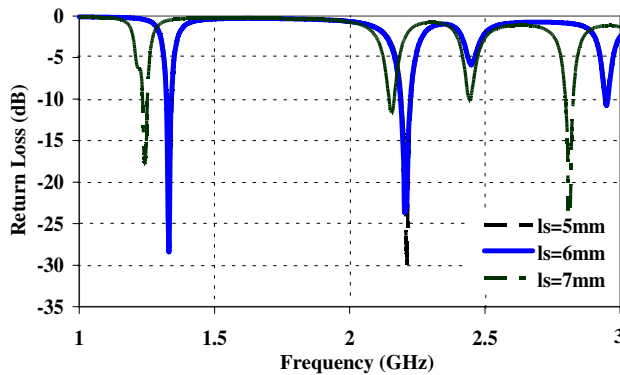


Figure 4. Return loss characteristics for different slot length values.

3.2. Effect of Slot Length (l_s)

In the next step, we tried to optimize the slot length, keeping the slot position obtained in Subsection 3.1. Here, the slot length was varied from 5 mm to 7 mm in steps of 1 mm. These characteristics are depicted in Figure 4. From the return loss characteristics it is clear that the slot length parameter (l_s) does not shift the frequency. However, it helps in optimizing the depth of S_{11} below -10 dB. From these characteristics it may be noted that the slot length of 6 mm exhibits optimum response.

3.3. Effect of Slot Width (w_s)

In the last step, slot width was varied from 31 mm to 34 mm in steps of 1 mm keeping $p = 15$ mm and $w_s = 32$ mm constant. The return loss characteristics for this case are presented in Figure 5. Like slot length this parameter helps in optimizing the depth of S_{11} curve.

From all the cases studied, the optimum set of slot dimensions is $p = 15$ mm, $l_s = 6$ mm, and $w_s = 32$ mm. Figure 6 depicts the radiation patterns obtained from the optimized geometry. As IE3D assumes infinite ground and substrate dimensions, the optimized geometry was re-simulated using Ansoft HFSS v.11 to test the cross and back lobe radiation effects. From these patterns it may be noted cross polarizations are well below -20 dB at the bore sight angle. Back lobe radiations are also acceptably low at both resonant frequencies. Also, at both resonant frequencies, more than 5 dB gain was observed.

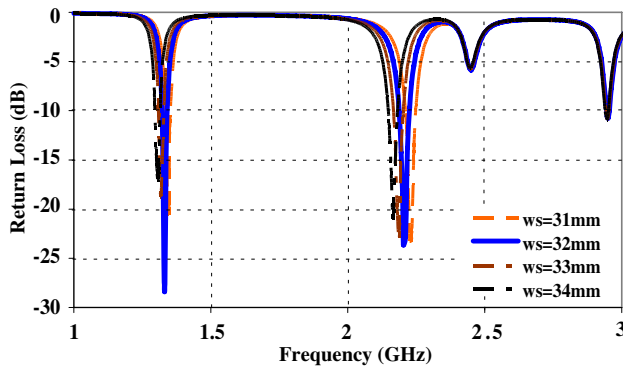


Figure 5. Return loss characteristics for different slot width values (other values are as listed in Table 1).

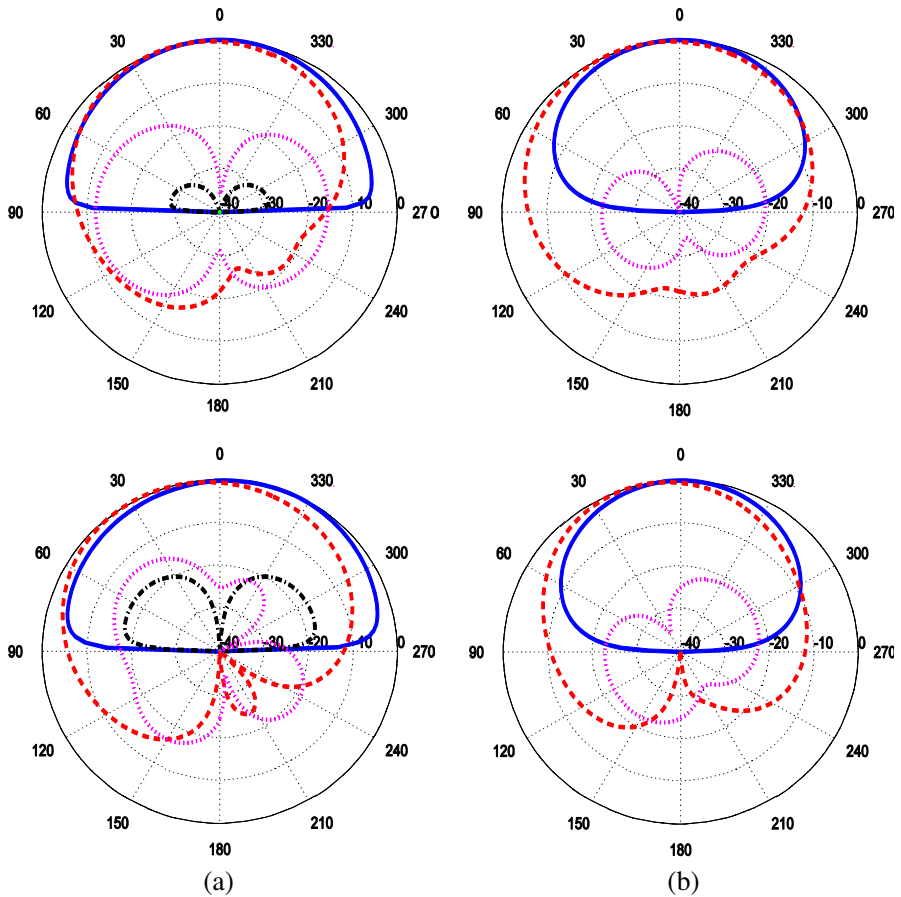


Figure 6. Radiation patterns of antenna without air gap (a) E -plane Co and Cross poln. patterns (left column) at first and second resonance frequencies. (b) H -plane Co and Cross poln. patterns (right column) at first and second resonance frequencies. Blue (solid curves): Co-poln. (IE3D); Red (dashed curves): Co-poln. (HFSS); Magenta (dotted curves): Cross poln. (IE3D); Black (dash-dot curves): Cross poln. (HFSS). Note: H-cross (right column: dash-dot curves (black)) is not visible as this curve is well below -40 dB.

4. EXPERIMENTAL RESULTS AND DISCUSSIONS

The prototype of the antenna with dimensions listed in Table 1 was fabricated (Figure 7(a)), and the return loss characteristics, and radiation patterns were measured. Return loss comparison plots

are shown in Figure 8(a). The measured and simulated gains are compared in Figure 9. Gain of the antenna is very high (nearly 8 dB) throughout the band of operation. The radiation patterns were measured in an anechoic chamber and plotted at first and

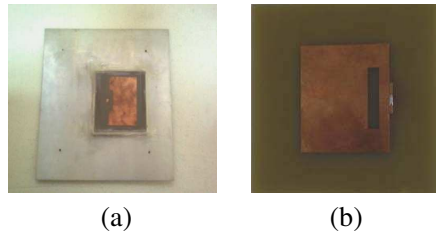


Figure 7. Fabricated prototypes. (a) Basic geometry. (b) Geometry without air gap.

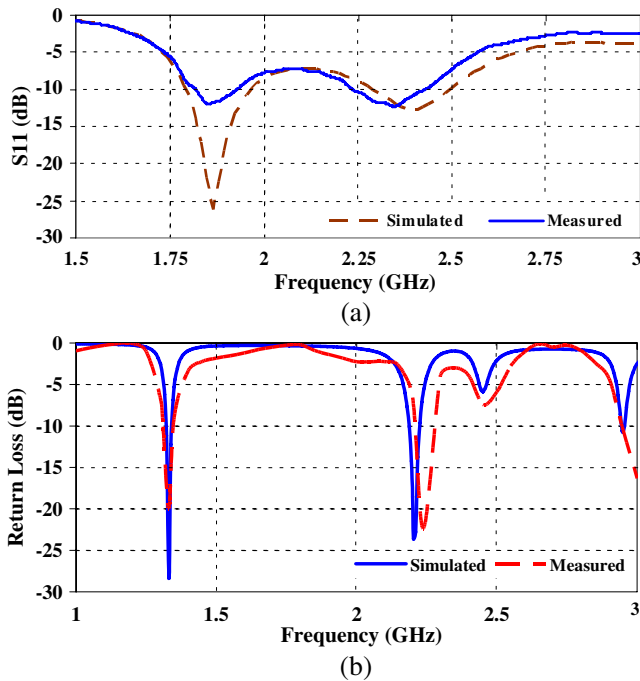


Figure 8. Return loss characteristics comparisons of antenna geometry shown in Figures 1 and 2. (a) Return loss characteristics of basic geometry. (b) Return loss characteristics of geometry without air gap.

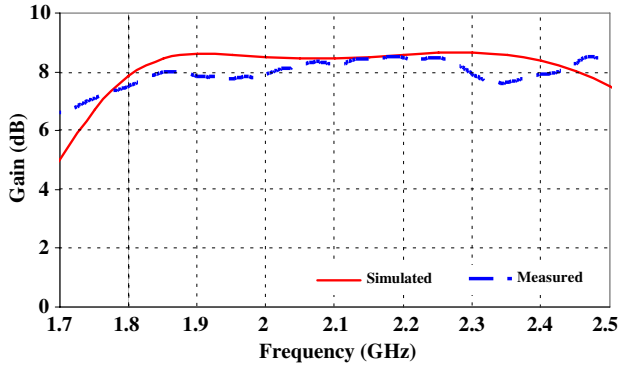


Figure 9. Gain vs. frequency of the basic antenna shown in Figure 1.

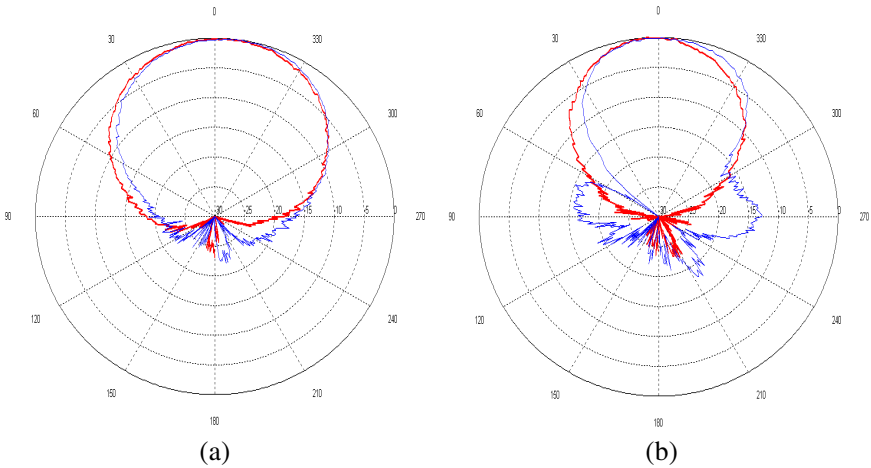


Figure 10. Measured radiation patterns at two resonant frequencies of antenna shown in Figure 1. (a) 1.8 GHz (b) 2.45 GHz.

second resonant frequencies as indicated in Figure 10. The fabricated prototype of geometry without air gap is depicted in Figure 7(b) and its return loss comparisons are presented in Figure 8(b). It may be noted from Figures 8(a) and (b) that the shift in the resonant frequency in the second case is due to the use of different substrate (dielectric constant) and absence of air gap. However, it may be redesigned to any frequency of interest as suggested in [9–15]. All measured results fairly agree with the simulated values.

5. CONCLUSIONS

The coplanar capacitive coupled probe fed microstrip antennas (with and without air gap) suitable for dual band wireless applications have been presented. The basic antenna uses small air gap offers dual bands with impedance bandwidths of 5.8% and 8.1% respectively, good radiation patterns, and high gain of about 8 dB in the bands of operation have been obtained. The air gap can be reduced about 55% compared to similar antenna designs reported earlier by cutting a slot within the radiating patch. Besides reducing the air gap, it (slot) also enables the antenna to operate at lower frequencies due to reactive loading. After presenting the basic geometry, the same configuration with no air gap was presented which also yields dual bands operation. The measured antenna characteristics are found to be in good agreement with the simulated results in the desired band of frequencies.

REFERENCES

1. Garg, R., P. Bhartia, I. Bahl, and A. Ittipiboon, *Microstrip Antenna Design Handbook*, Artech House, Norwood, MA, 2001.
2. Kumar, G. and K. P. Ray, *Broadband Microstrip Antennas*, Artech House, 2003.
3. Luk, K. M., K. F. Lee, and W. L. Tam, "Circular U-slot patch with dielectric superstrate," *Electronics Letters*, Vol. 33, No. 12, 1001–1002, 1997.
4. Ooi, B. L. and I. Ang, "Broadband semicircle fed flower-shaped microstrip patch antenna," *Electron. Lett.*, Vol. 41, No. 17, 2005.
5. Targonski, S. D., R. B. Waterhouse, and D. M. Pozar, "Wideband aperture coupled stacked patch antenna using thick substrates," *Electronics Letters*, Vol. 32, No. 21, 1941–1942, 1996.
6. Lai, H. W. and K. M. Luk, "Wideband stacked patch antenna fed by meandering probe," *Electron. Lett.*, Vol. 41, No. 6, 2005.
7. Mak, C. L., K. F. Lee, and K. M. Luk, "A novel broadband patch antenna with a T-shaped probe," *IEE Proc. Microw., Antennas Propagat.*, Part H, Vol. 147, 73–76, 2000.
8. Mayhew-Ridgers, G., J. W. Odendaal, and J. Joubert, "Single-layer capacitive feed for wideband probe-fed microstrip antenna elements," *IEEE Trans. Antennas Propagat.*, Vol. 51, 1405–1407, 2003.
9. Kasabegoudar, V. G., D. S. Upadhyay, and K. J. Vinoy, "Design

- studies of ultra wideband microstrip antennas with a small capacitive feed," *Int. J. Antennas Propagat.*, 1–8, 2007.
10. Kasabegoudar, V. G. and K. J. Vinoy, "A wideband microstrip antenna with symmetric radiation patterns," *Microw. Opt. Technol. Lett.*, Vol. 50, No. 8, 1991–1995, 2008.
 11. Kasabegoudar, V. G. and K. J. Vinoy, "Coplanar capacitively coupled probe fed microstrip antennas for wideband applications," *IEEE Trans. Antennas Propagat.*, Vol. 58, No. 10, 3131–3138, 2010.
 12. Kasabegoudar, V. G. and K. J. Vinoy, "A broadband suspended microstrip antenna for circular polarization," *Progress In Electromagnetics Research*, Vol. 90, 353–368, 2009.
 13. Kasabegoudar, V. G. and K. J. Vinoy, "A coplanar capacitively coupled probe fed microstrip antenna for wireless applications," *The 2009 International Symposium on Antennas and Propagation*, 297–300, 2009.
 14. Kasabegoudar, V. G., "Dual frequency ring antenna with capacitive feed," *Progress In Electromagnetics Research C*, Vol. 23, 27–39, 2011.
 15. Kasabegoudar, V. G., "Low profile suspended microstrip antennas for wideband applications," *Journal of Electromagnetic Waves and Applications*, Vol. 25, No. 13, 1795–1806, 2011.
 16. Schellenberg, J. M., "CAD models for suspended and inverted microstrip," *IEEE Trans. Microw. Theory and Tech.*, Vol. 43, No. 6, 1995.
 17. Anguera, J., C. Puente, and C. Borja, "Dual frequency broadband microstrip antenna with a reactive loading and stacked elements," *Progress in Electromagnetics Research Letters*, vol. 10, 1–10, 2009.
 18. Mayhew-Rydgers, G., J. W. Avondale, and J. Joubert, "New feeding mechanism for annular-ring microstrip antenna," *Electronics Letters*, Vol. 36, 605–606, 2000.
 19. Sze, J. Y., T. H. Hu, and T. J. Chen, "Compact dual-band annular-ring slot antenna with meandered grounded strip," *Progress In Electromagnetics Research*, Vol. 95, 299–308, 2009.
 20. Lee, B. M. and Y. J. Yoon, "A dual fed and a dual frequency slots loaded triangular microstrip antenna," *IEEE Antenna and Propagation Society Int. Symp.*, Vol. 3, 1600–1603, 2000.
 21. Ren, W., "Compact dual-band slot antenna for 2.4/5 GHz WLAN applications," *Progress In Electromagnetics Research B*, Vol. 8, 319–327, 2008.
 22. Su, C. W., J. S. Row, and J. F. Wu, "Design of a single feed dual-

- frequency microstrip antenna,” *Microw. Opt. Technol. Letters*, Vol. 47, No. 2, 114–116, 2005.
23. Liao, W. and Q.-X. Chu, “Dual-band circularly polarized microstrip antenna with small frequency ratio,” *Progress In Electromagnetics Research Letters*, Vol. 15, 145–152, 2010.
 24. Alkanhal, M. A. and A. F. Sheta, “A novel dual-band reconfigurable square-ring microstrip antenna,” *Progress In Electromagnetic Research*, Vol. 70, 337–349, 2007.
 25. Chen, H.-M., “Single-feed dual-frequency rectangular microstrip antenna with a π -shaped slot,” *IEE Proc. — Microw. Antennas Propag.*, Vol. 148, No. 1, 60–64, 2001.
 26. Arya, A. K., A. Patnaik, and M. V. Kartikeyan, “Microstrip patch antenna with skew-F shaped DGS for dual band operation,” *Progress In Electromagnetics Research M*, Vol. 19, 147–160, 2011.
 27. Yuan, H., J. Zhang, S. Qu, H. Zhou, J. Wang, H. Ma, and Z. Xu, “Dual-band dual polarized microstrip antenna for compass navigation satellite system,” *Progress In Electromagnetics Research C*, Vol. 30, 213–223, 2012.
 28. Zhuo, Y., L. Yan, X. Zhao, and K.-M. Huang, “A compact dual-band patch antenna for WLAN applications,” *Progress In Electromagnetics Research Letters*, Vol. 26, 153–160, 2011.
 29. Liu, W.-C. and Y. Dai, “Dual-broadband twin-pair inverted-L shaped strip antenna for WLAN/WiMAX applications,” *Progress In Electromagnetics Research Letters*, Vol. 27, 63–73, 2011.
 30. Li, W.-M., Y. Jiao, and D. Li, “Dual-band circularly polarized slot antenna for WiMAX/WLAN application,” *Progress In Electromagnetic Research Letters*, Vol. 33, 101–108, 2012.